

EPJ D

Atomic, Molecular,
Optical and Plasma Physics

EPJ.org

your physics journal

Eur. Phys. J. D **56**, 199–203 (2010)

DOI: 10.1140/epjd/e2009-00298-x

Non-jellium scaling of metal cluster ionization energies and electron affinities

M. Svanqvist and K. Hansen



Non-jellium scaling of metal cluster ionization energies and electron affinities

M. Svanqvist¹ and K. Hansen^{2,a}

¹ Department of Physics, University of Freiburg, Stefan-Meier-Straße 19, 79104 Freiburg, Germany

² Department of Physics, University of Gothenburg, SE-412 96 Göteborg, Sweden

Received 6 February 2009 / Received in final form 7 June 2009

Published online 24 November 2009 – © EDP Sciences, Società Italiana di Fisica, Springer-Verlag 2009

Abstract. Experimental literature data on ionization energies and electron affinities of metal clusters are reviewed and analyzed in terms of an expansion in the inverse cluster radius. The coefficient of the finite size correction for ionization energies decreases with increasing bulk work function whereas the corresponding coefficient for electron affinities increases. This sharply contrasts the predictions based both on density functional theory of spherical jellium clusters and on classical electrostatics. A scaling of the coefficient for the ionization potentials with the atomic radius yields a linear behavior which extrapolates to zero around 6 eV.

PACS. 36.40.-c Atomic and molecular clusters – 33.15.Ry Ionization potentials, electron affinities, molecular core binding energy – 33.80.Eh Autoionization, photoionization, and photodetachment

1 Introduction

The scaling of cluster ionization energies, IEs (or ionization potentials, IPs) with cluster size is generally recognized as having the form of a constant, usually identified with the bulk work function, plus a positive term proportional to the reciprocal radius of the cluster,

$$IE_N = b + \frac{\alpha}{R_N} = b + a \frac{e^2}{4\pi\epsilon_0 r_1} N^{-1/3}, \quad (1)$$

where N is the number of atoms in the cluster, r_1 is the radius of the atom calculated from the bulk number density, n , as

$$\frac{4\pi}{3} r_1^3 = n^{-1}. \quad (2)$$

Electron affinities (EA) are analyzed with an equation similar to that of the IE's;

$$EA_N = b - \frac{\beta}{R_N} = b - c \frac{e^2}{4\pi\epsilon_0 r_1} N^{-1/3}. \quad (3)$$

The value and interpretation of the constant term b as the bulk work function is rarely disputed. The formulation of the dependence in terms of the factor a for the ionization energies in equation (1) and the corresponding factor c for the electron affinities (EA) in equation (3) emphasizes the interpretation of the size dependent term as deriving from electrostatics. The magnitudes of these two dimensionless parameters are on the order of unity, lending credibility to this interpretation.

Three different suggestions for the values of a can be found in the literature, predicting either a single or a set of values [1–10]. The value $a = 1/2$ is derived from the capacitance of a metallic sphere. The alternative classical value $a = 3/8$ is derived with a calculation of the polarization energy of the system composed of metal sphere and electron, and arises after the initial, divergent expression is regularized by forming the difference between two identical infinities. Surprisingly, there is still no consensus on the correct value of this purely classical quantity. Experimental values are influenced also by quantum corrections which act to reduce the value with a material dependent term. The third class of suggestions include such corrections explicitly by taking into account the quantum nature of the valence electrons in metal clusters. Values are typically calculated with density functional theory (DFT) [11–13].

The purpose of this work is to attempt an unbiased analysis of the existing experimental data to provide an improved empirical basis for a more fundamental understanding of the finite size scaling relation, in particular with respect to the predictions of jellium descriptions of metal clusters.

2 Data analysis

The data used in the present analysis are previously published results on ionization energies and electron affinities of pure metal clusters, specified with respect to cluster size. For comparison, semiconductor and semimetal clusters are also included in the study. Most of the data used

^a e-mail: klavs@physics.gu.se

Table 1. The parameters a , b derived from fitting of experimental data to equation (1). The values of W_∞ are from [14]. Superscript indicates method: ¹photoionization, ²electron impact ionization and ³charge transfer reaction. Some uncertainty is associated with the work function of Pr.

Element	Size range [Ref.]	a	b [eV]	W_∞/b
Li ¹	2–26 [15]	0.41 ± 0.08	2.05 ± 0.32	1.43
C ³	6–100 sparse [16,17]	0.56 ± 0.14	5.53 ± 0.58	0.90
Na ¹	2–22 [18]	0.28 ± 0.10	2.96 ± 0.35	0.80
Na ¹	9–80 [19]	0.28 ± 0.03	2.86 ± 0.05	0.83
Al ¹	2–53 [20]	0.40 ± 0.05	4.24 ± 0.17	0.98
Si ¹	2–45 [21]	0.92 ± 0.14	3.49 ± 0.49	1.26
K ¹	3–30 [22]	0.30 ± 0.06	2.37 ± 0.15	0.97
V ¹	2–22 [23]	0.31 ± 0.02	3.68 ± 0.10	1.17
Cr ¹	4–25 [24]	0.26 ± 0.06	4.07 ± 0.14	1.11
Mn ¹	7–64 [25]	0.30 ± 0.04	3.74 ± 0.13	1.10
Fe ¹	6–90 [26]	0.22 ± 0.01	4.47 ± 0.05	1.06
Co ¹	3–92 [26]	0.16 ± 0.03	4.98 ± 0.09	1.00
Ni ¹	3–90 [27]	0.10 ± 0.01	5.46 ± 0.02	0.92
Cu ¹	3–122 [28]	0.25 ± 0.04	4.62 ± 0.12	1.05
Ge ¹	2–57 [29]	0.77 ± 0.09	3.90 ± 0.28	1.28
Y ¹	2–31 [30]	0.33 ± 0.03	3.11 ± 0.10	1.00
Nb ¹	2–76 [31]	0.29 ± 0.03	3.94 ± 0.10	1.09
Ag ¹	3–100 [32]	0.32 ± 0.08	3.88 ± 0.21	1.19
Ag ²	2–36 [33]	0.28 ± 0.09	5.22 ± 0.37	0.89
Cd ¹	2–30 [34]	0.65 ± 0.07	3.54 ± 0.27	1.15
Sn ¹	2–41 [29]	0.58 ± 0.09	4.43 ± 0.28	1.00
Ta ¹	2–64 [35]	0.21 ± 0.02	4.22 ± 0.08	1.01
Au ²	3–22 [36]	0.34 ± 0.20	6.46 ± 0.90	0.83
Hg ¹	2–109 [37]	0.89 ± 0.10	4.42 ± 0.58	1.01
Bi ¹	2–38 [38]	0.63 ± 0.06	4.58 ± 0.18	0.92
Ce ¹	2–21 [39]	0.26 ± 0.09	3.27 ± 0.35	0.89
Pr ¹	2–17 [39]	0.19 ± 0.04	3.54 ± 0.13	0.77

are available in tabulated form from the original publications. For the remaining, they were digitized from the published graphs. For each species, the experimental data are fitted using the least squares method, including all measured points (but excluding the monomer) and with equal weight to each point. All atomic radii are calculated from tabulated densities at 20 °C. For carbon the density of graphite was used. Data sets covering only the smallest sizes, below $N \approx 15$, are excluded to avoid distortion of the fits from shell- and odd-even effects. Data on mixed clusters are not included because size dependence in general is an ambiguous concept for these.

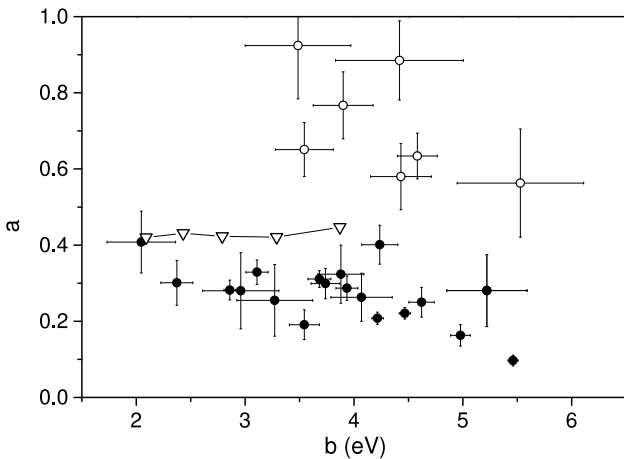
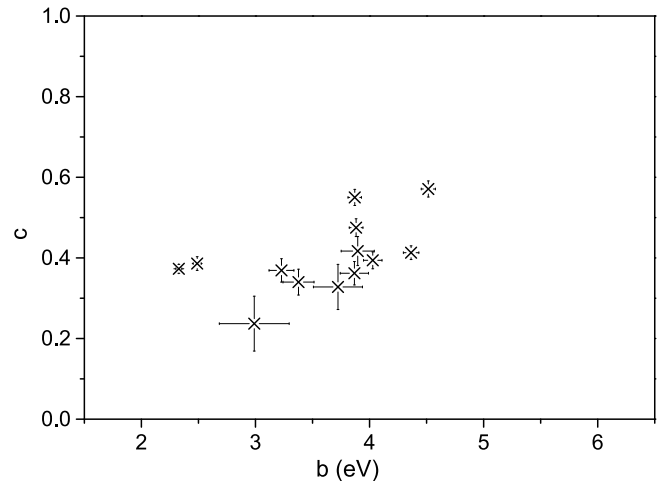
The quantity b in equation (1) is, as mentioned, equated with the bulk work function, W , but since b is a fitted parameter it may differ from tabulated values of W . The agreement between W and b is reasonable, although not perfect. The comparison is given in Table 1 together with the fitted values of a . The values of c and b (Eq. (3)) are given in Table 2. Since the values of the b 's derive from fits they are not necessarily identical for the same element for electron affinities and ionization energies. This may in part be due to the difference between

the electron affinity/ionization energy and the vertical detachment energy, which is the quantity measured in the experiments. In total, there are data for the IE's and EA's for five elements (Na, Al, Cu, Ag, and Hg). Of these, either the IE or the EA has been determined twice in three cases (Na, Al, and Ag). The mean of the absolute relative difference between the two determinations of IE or EA for these three elements is 0.12. This should be compared with the similar number when IE and EA are compared, which is 0.19. These two numbers are similar and do not give us reason to suggest that the ionization energies and the electron affinities extrapolate to different work functions. It requires a much larger sample to reveal any systematic trend of this kind. We note that the trend towards a deviation from the DFT-jellium calculations which will be discussed below was present for these fits also.

The ionization energies for clusters of different elements have been determined for different size ranges and fits could potentially introduce spurious correlations between the values of a and b , depending on the precise size range used. These correlations appear for example if higher order terms in $N^{-1/3}$ are important in the

Table 2. The parameters c , b derived from fitting of experimental data on photodetachment energies to equation (3). The values of W_∞ are from [14].

Element	Size range [Ref.]	c	b [eV]	W_∞/b
Na	2–110 [40]	0.39 ± 0.02	2.49 ± 0.04	0.95
Mg	3–95 [40]	0.55 ± 0.02	3.87 ± 0.06	1.13
Al	3–32 [41]	0.39 ± 0.02	4.03 ± 0.08	1.04
Al	2–25 [42]	0.36 ± 0.03	3.87 ± 0.12	1.08
Cu	6–41 [43]	0.33 ± 0.06	3.72 ± 0.22	1.3
Zn	3–117 [40]	0.57 ± 0.02	4.52 ± 0.06	1.13
Sr	2–56 [40]	0.37 ± 0.01	2.33 ± 0.03	1.10
Ag	2–21 [44]	0.24 ± 0.07	2.99 ± 0.31	1.55
In	2–15 [45]	0.34 ± 0.03	3.38 ± 0.14	1.21
W	2–90 sparse [46]	0.42 ± 0.04	3.90 ± 0.15	1.17
Re	2–40 [47]	0.41 ± 0.02	4.36 ± 0.07	1.08
Hg	3–383 sparse [48]	0.81 ± 0.02	4.83 ± 0.05	0.93
Tl	2–20 [45]	0.37 ± 0.03	3.23 ± 0.11	1.19
Pb	3–204 sparse [49]	0.48 ± 0.02	3.88 ± 0.06	1.09

**Fig. 1.** Fitted values of a vs. b . filled circles indicate metallic elements, open circles the semi metals/semiconductors. The open triangles are the calculated values from [13].**Fig. 2.** Fitted values of c vs. b . The elements are Cu, Ag, In, W, Re, Tl, Pb, Al, Mg, Zn, Sr, Na.

expansion in equation (1). No such correlation was seen in a plot of a vs. $N_l^{-1/3} - N_h^{-1/3}$, where N_l, N_h are the lowest and highest sizes in the individual data sets. Such artifacts caused by the fitting can therefore be ruled out.

The values of a appear to fall in two bands when plotted vs. b , as seen in Figure 1, one for metals and one for semimetals/semiconductors. The two groups are Li, Na, K, Al, Cr, Mn, Fe, Co, Ni, Y, Nb, Ce, Cu, Ag, Pr, Ta, V, and Hg, Si, Ge, Cd, Sn, C, Bi. One point (on Au) is excluded from the figure because the 1σ error bars exceeded 50% of the value itself. The values for metals are almost all at or below 0.3, with a tendency to decrease with increasing work function. The trend is similar for the semimetals but the values are more than twice the values for metals for the same value of b . The tendency for a to decrease with b differs radically from earlier compilations, (see e.g. [50]) where IEs were fitted with a constant value of a .

Mercury is often used as a paradigm of a transition from Van der Waals binding at small cluster sizes to metallic structure at larger clusters [51] (although it has been argued that this viewpoint needs modifications [48]). One will therefore expect to see different sets of values of a , b for small and for large clusters. This is indeed also found, but surprisingly both points lie on the curve corresponding to semimetals, albeit with different positions on the curve. For this reason we did not distinguish between large and small and used a single value for mercury, fitted over all sizes measured.

A plot has been made (not shown) with the data fitted with a cluster radius given by $r_1 N^{1/3} + \Delta r$ where Δr is the so-called spill-out. The results are quite similar to Figures 1 and 2, although individual points shift by small amounts along the curve.

Figure 2 shows the coefficient c related to the scaling of the electron affinities. We note a tendency to an increase

of c with work function, although this is partly obscured by the scatter in the data. This is the opposite trend of that for a . To the extent that these trends apply to IE's and EA's of the same elements, they indicate that the size independent relation $IE_N + EA_N \approx 2W$ given in [52] (for Al and K) does not hold generally. This relation would require that $a \approx c$.

A striking correlation between fitted values is found if instead of a and c , ar_1 and $(1-c)r_1$ for the metals are plotted vs. the work functions, see Figure 3. The variations of both ar_1 and $(1-c)r_1$ with b appear to be linear and both extrapolate to zero at values between 6 and 6.5 eV. The trend of a decreasing value of ar_1 with increasing b is partly due to the inverse relationship between r_1 and b for simple Fermi gases. The appearance of a linear behavior for both the IEs and the EAs is the most surprising feature of the data. We note that work functions above 6 eV are rare, and none are listed in e.g. [53] or [14]. The implications of this are not clear to us at present, although a violation of this apparent $W < 6$ eV rule would have interesting consequences for plasma- and cluster physics.

3 Discussion

The quantum corrections to the electrostatic values of a have been investigated by several authors, see e.g. [11–13]. In [13] calculations were performed on clusters in which the ionic cores were described as jellium and the electrons with density functional theory. The corrections were found to be typically -0.08 for the high densities and slightly closer to zero for the highest density calculated which corresponded to a Wigner-Seitz radius of $2a_0$. Also the work functions were calculated and these data are included in Figure 1. The calculated effect is too small to account for the observed effect, and furthermore has an incorrect trend as a function of work function.

We ascribe the discrepancy to the approximations involved in the jellium description. Although jellium-based models have successfully described an impressive range of phenomena in metal clusters, in particular for alkali metal clusters, most of these do not depend critically on the properties of cluster surfaces. The quantum corrections to ionization energies, on the other hand, depend critically on the charge distribution at the cluster surface and will be influenced by the granularity of the surface. The magnitude of this effect depends on the element.

It is generally believed that the variation of the c parameter describing the size dependence of the electron affinity is opposite to that of the ionization energy, parameterized as [54]

$$a = 1/2 - \delta, \quad c = 1/2 + \delta, \quad (4)$$

for the same material. Although the trend is confirmed here in the sense that a larger ar_1 gives a larger $(1-c)r_1$, the different slopes of the electron affinity data and the ionization energy data suggest that $a + c$ is not unity

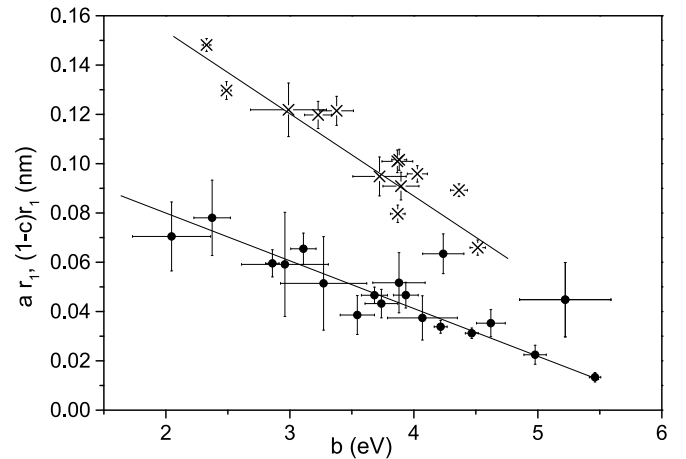


Fig. 3. ar_1 (filled circles) and $(1-c)r_1$ (crosses) vs. b . Only the metallic elements are included. One of the two high points on ionization energies, at $b = 5.2$ eV, is from data recorded with electron impact ionization. This ionization method tends to give high values for a 's, and the data point is higher than the corresponding photoionization data for the same elements. The lines are guides to the eye.

and not even a constant [11]. Judged by the slopes in Figure 3, which have a ratio of approximately 1:2, and identical intercept with the abscissa, the relation is rather $2a \approx c$. From Figure 3 the scaling relation for a is found to be

$$a = \frac{0.11 \text{ nm}}{r_1} - \frac{0.018 \text{ nm}}{r_1} \frac{b}{\text{eV}}, \quad (5)$$

and for c

$$c = -\frac{0.23 \text{ nm}}{r_1} + 1 + \frac{0.035 \text{ nm}}{r_1} \frac{b}{\text{eV}}. \quad (6)$$

These equations constitute quantitative predictions for the values of a and c for hitherto unmeasured metallic elements.

4 Conclusions

The analysis presented here suggests that for metal clusters a scaling exists for the parameters of the expansion of the ionization energies in the reciprocal radius. It provides non-trivial predictions for as yet unmeasured quantities. The results presented here show that the predictions from literature based on density functional theory calculations with the positive background treated as a jellium fail. We stress that this is not a failure of the density functional theory, but of the jellium description of the clusters.

This work was supported by the Swedish National Research Council (VR). Comments by M. Manninen, V.V. Kresin and O. Echt are gratefully acknowledged.

References

1. F.T. Smith, *J. Chem. Phys.* **34**, 793 (1961)
2. J.M. Smith, *AAIA J.* **3**, 648 (1965)
3. D.M. Wood, *Phys. Rev. Lett.* **46**, 749 (1981)
4. L.E. Brus, *J. Chem. Phys.* **79**, 5566 (1983)
5. G. Makov, A. Nitzan, L.E. Brus, *J. Chem. Phys.* **88**, 5076 (1988)
6. J.P. Perdew, *Phys. Rev. B* **37**, 6175 (1988)
7. W.A. de Heer, P. Milani, *Phys. Rev. Lett.* **65**, 3356 (1990)
8. M.K. Harbola, *J. Chem. Phys.* **97**, 2578 (1992)
9. M. Seidl, J.P. Perdew, *Phys. Rev. B* **50**, 5744 (1994)
10. S. Halas, *Chem. Phys. Lett.* **370**, 300 (2003)
11. M. Seidl, K.-H. Meiwes-Broer, M. Brack, *J. Chem. Phys.* **95**, 1295 (1991)
12. M. Seidl, J.P. Perdew, M. Brajczewska, C. Fiolhais, *Phys. Rev. B* **55**, 13288 (1997)
13. M. Seidl, J.P. Perdew, M. Brajczewska, C. Fiolhais, *J. Chem. Phys.* **108**, 8182 (1998)
14. *CRC Handbook of Chemistry and Physics*, edited by D.R. Lide, 87th edn. (2006-2007)
15. P. Dugourd et al., *Chem. Phys. Lett.* **197**, 433 (1992)
16. S.B.H. Bach, J.R. Eyler, *J. Chem. Phys.* **92**, 358 (1990)
17. J.A. Zimmerman, J.R. Eyler, S.B.H. Bach, S.W. McElvany, *J. Chem. Phys.* **94**, 3556 (1991)
18. M.M. Kappes et al., *Chem. Phys. Lett.* **143**, 251 (1988)
19. J.L. Persson, Thesis, University of California, 1991
20. K.E. Schriver, J.L. Persson, E.C. Honea, R.L. Whetten, *Phys. Rev. Lett.* **64**, 2539 (1990)
21. K. Fuke, K. Tsukamoto, F. Misaizu, M. Sanekata, *J. Chem. Phys.* **99**, 7807 (1993)
22. W.A. Saunders, K. Clemenger, W.A. de Heer, W.D. Knight, *Phys. Rev. B* **32**, 1366 (1985)
23. A. Kaldor, D.M. Cox, D.J. Trevor, M.R. Zakin, *Z. Phys. D* **3**, 195 (1986)
24. M.B. Knickelbein, *Phys. Rev. A* **67**, 013202 (2003)
25. G.M. Koretsky, M.B. Knickelbein, *J. Chem. Phys.* **106**, 9810 (1997)
26. S. Yang, M.B. Knickelbein, *J. Chem. Phys.* **93**, 1533 (1990)
27. M.B. Knickelbein, S. Yang, S.J. Riley, *J. Chem. Phys.* **93**, 94 (1990)
28. M.B. Knickelbein, *Chem. Phys. Lett.* **192**, 129 (1992)
29. S. Yoshida, K. Fuke, *J. Chem. Phys.* **111**, 3880 (1999)
30. M.B. Knickelbein, *J. Chem. Phys.* **102**, 1 (1995)
31. M.B. Knickelbein, S. Yang, *J. Chem. Phys.* **93**, 5760 (1990)
32. G. Alameddine, J. Hunter, D. Cameron, M.M. Kappes, *Chem. Phys. Lett.* **192**, 122 (1992)
33. C. Jackschath, I. Rabin, W. Schulze, *Z. Phys. D* **22**, 517 (1992)
34. M. Ruppel, K. Rademann, *Chem. Phys. Lett.* **192**, 280 (1992)
35. B.A. Collings, D.M. Rayner, P.A. Hackett, *Int. J. Mass Spectrom. Ion Proc.* **125**, 207 (1993)
36. C. Jackschath, I. Rabin, W. Schulze, *Ber. Bunsenges. Phys. Chem.* **96**, 1200 (1992)
37. K. Rademann, *Z. Phys. D* **19**, 161 (1991)
38. R.E. Walstedt, R.F. Bell, *Phys. Rev. A* **33**, 2830 (1986)
39. G.M. Koretsky, M.B. Knickelbein, *Eur. Phys. J. D* **2**, 273 (1998)
40. O. Kostko, Thesis, University of Freiburg, 2007
41. K.J. Taylor et al., *Chem. Rev. Lett.* **152**, 347 (1988)
42. G. Ganteför, M. Gausa, K.H. Meiwes-Broer, H.O. Lutz, *Z. Phys. D* **9**, 253 (1988)
43. C.L. Pettiette et al., *J. Chem. Phys.* **88**, 5377 (1988)
44. G. Ganteför, M. Gausa, K.H. Meiwes-Broer, H.O. Lutz, *J. Chem. Soc. Faraday Trans.* **86**, 2483 (1990)
45. M. Gausa, G. Ganteför, H.O. Lutz, K.H. Meiwes-Broer, *Int. J. Mass Spectrom. Ion Proc.* **102**, 227 (1990)
46. G.H. Lee et al., *Chem. Phys. Lett.* **299**, 309 (1999)
47. A. Pramann, K. Rademann, *Chem. Phys. Lett.* **347**, 46 (2001)
48. R. Busani, M. Folkers, O. Cheshnovsky, *Phys. Rev. Lett.* **81**, 3836 (1998)
49. Ch. Lüder, K.H. Meiwes-Broer, *Chem. Phys. Lett.* **294**, 391 (1998)
50. M.M. Kappes, *Chem. Rev.* **88**, 369 (1988)
51. K. Rademann, B. Kaiser, U. Even, F. Hensel, *Phys. Rev. Lett.* **59**, 2319 (1987)
52. W.A. de Heer, *Rev. Mod. Phys.* **65**, 611 (1993)
53. H.B. Michaelson, *J. Appl. Phys.* **48**, 4729 (1977)
54. E. Engel, J.P. Perdew, *Phys. Rev. B* **43**, 1331 (1991)